JOURNAL OF GEOPHYSICAL RESEARCH, VOL. 112, F04007, doi:10.1029/2006JF000731, 2007

Tides and the flow of Rutford Ice Stream, West Antarctica

G. Hilmar Gudmundsson[1]

Received 30 November 2006; revised 27 April 2007; accepted 2 August 2007; published 15 November 2007.

[1] Surface speeds of Rutford Ice Stream, West Antarctica, are known to vary by around 10–20% (depending on location) with a fortnightly periodicity corresponding to a spring-neap tidal cycle. The reasons for these periodic variations in flow are unclear. Here the possible role of tidal stress transmission upstream of the grounding line in affecting rates of basal motion is investigated. It is found that nonlinear rheological effects within the till, when coupled with transmission of tidal stresses within the ice that are linearly related to tidal amplitude, can give rise to the type of periodic oscillations in flow observed. This nonlinear interaction between tidal forcing and till deformation increases the mean ice flux across the grounding line by a few percent above what might be expected in the absence of tidal forcing. Periodic velocity fluctuations of this type have not been observed on other ice streams. However, modeling suggests that this may be due to lack of data and that such flow variations are likely to be common features of active ice streams draining into the Ronne Ice Shelf, as well as of other ice streams subjected to similar tidal forcing.

Citation: Gudmundsson, G. H. (2007), Tides and the flow of Rutford Ice Stream, West Antarctica, *J. Geophys. Res.*, *112*, F04007, doi:10.1029/2006JF000731.

1. Introduction

[2] Flow speeds of ice streams far inland from the grounding line can be significantly affected by tides. Examples for such flow variations have been found on the ice plain of Whillans Ice Stream [*Bindschadler et al.*, 2003a, 2003b], on Bindschadler Ice Stream [*Anandakrishnan and Alley*, 1994; *Anandakrishnan et al.*, 2003], on Kamb Ice Stream [*Anandakrishnan and Alley*, 1997], and on Rutford Ice Stream [*Gudmundsson*, 2006]. These observations of tidally induced fluctuations in speed show that tidal effects are of long range and not limited to a few km zone around the grounding line as had previously been implicitly assumed when modeling tidal effects on ice streams [e.g., *Doake et al.*, 1987; *Smith*, 1991; *Vaughan*, 1995]. The temporal pattern of tidal modulation varies greatly between ice streams. On the ice plain of Whillans Ice Stream stick-slip motion was observed [*Bindschadler et al.*, 2003a], while flow velocities of Bindschadler Ice Stream vary smoothly by a factor of three over each diurnal tidal cycle [*Anandakrishnan et al.*, 2003]. A different type of behavior is seen on Rutford Ice Stream with velocities varying about 20% over a period corresponding to a spring-neap tidal cycle [*Gudmundsson*, 2006]. There is an indication of diurnal variations in near-surface vertical strain and seismicity more than 300 km up stream from the grounding line of Whillans Ice Stream [*Harrison et al.*, 1993], and on Kamb Ice Stream tides affect basal seismicity far inland [*Anandakrishnan and Alley*, 1997].

[3] Here it is shown how a simple model can give rise to fortnightly variations in flow of the type observed on Rutford Ice Stream. The model arises from two basic assumptions: (1) within the ice, tidally induced stress perturbations are linearly related to tidal amplitude, and (2) deformation of till follows a nonlinear relationship between shear stress and rates of basal motion. The first assumption is that of linear viscoelasticity over timescales of hours and a few days, and the second one is that of nonlinear viscous response of till to applied stresses. Although no direct comparison with data from other ice streams is attempted, sensitivity analysis suggests that some of the observed differences in tidal flow variations between Rutford Ice Stream and Bindschadler Ice Stream are due to differences in tidal forcing rather than differences in ice or till rheology.

2. Data

[4] Over the time period from late December 2003 to mid February 2004, five GPS receivers were operated continuously on Rutford Ice Stream (78°S, 83°W), West Antarctica. Site locations are shown in Figure 1. The stations were all located along the medial line with one station some 20 km downstream from the grounding line (R-20), another one at the grounding line (R+00), and further three stations some 10, 20, and 40 km upstream from the grounding line (R+10, R+20, R+40). GPS observations were made every 10 sec. These observations were preprocessed and kinematic single-epoch point positions calculated every 5 min using the Bernese GPS software [*Hugentobler et al.*, 2006]. Ocean loading corrections were made using GOT00.2 (http://www.oso.chalmers.se/~loading). For discussion of the importance of ocean loading corrections and issues related to

[1]British Antarctic Survey, Cambridge, UK.

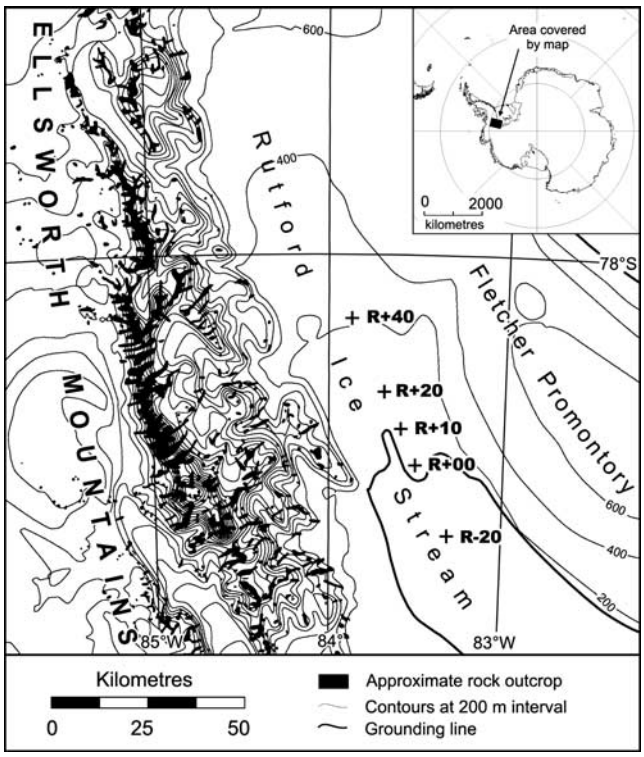

Figure 1. Map of Rutford Ice Stream showing the location of GPS sites. Overall flow direction of Rutford Ice Stream is from top left to bottom right.

accurate GPS processing in polar regions see *King et al.* [2000] and *King* [2004].

[5] Detrended in-line positions at stations R+00, R+20, and R+40 are shown in Figure 2 (thick red lines). The thin black curves in Figure 2 are modeled position and will be discussed in detail below. At all sites a periodic variation in detrended in-line displacement with a fortnightly periodicity is seen. Superimposed on the fortnightly period are smaller semidiurnal variations. The amplitude of the semidiurnal variation changes over each fortnightly period, with large semidiurnal amplitudes during an increase in the fortnightly component, and small semidiurnal amplitudes during a corresponding decrease in the slope of the fortnightly variation. A comparison with the tidal record from R-20 revealed that large semidiurnal horizontal in-line amplitudes closely coincide with a spring tide, and the small semidiurnal amplitudes with the ocean neap tide. In terms of velocity of the ice stream, this implies maximum and minimum fortnightly velocities are roughly in phase with spring and neap tides, respectively. The exact phase relationship will be discussed in more detail below.

[6] The variation in velocity (slopes of the curves in Figure 2) are thus clearly related to, and presumably driven by, the ocean tides. The phase relationship is hence best analyzed by considering the relative phase shift of each tidal component of the in-line horizontal variation with respect to the corresponding component of the vertical ocean tide. This is shown in Figure 3 where these relative phase shifts

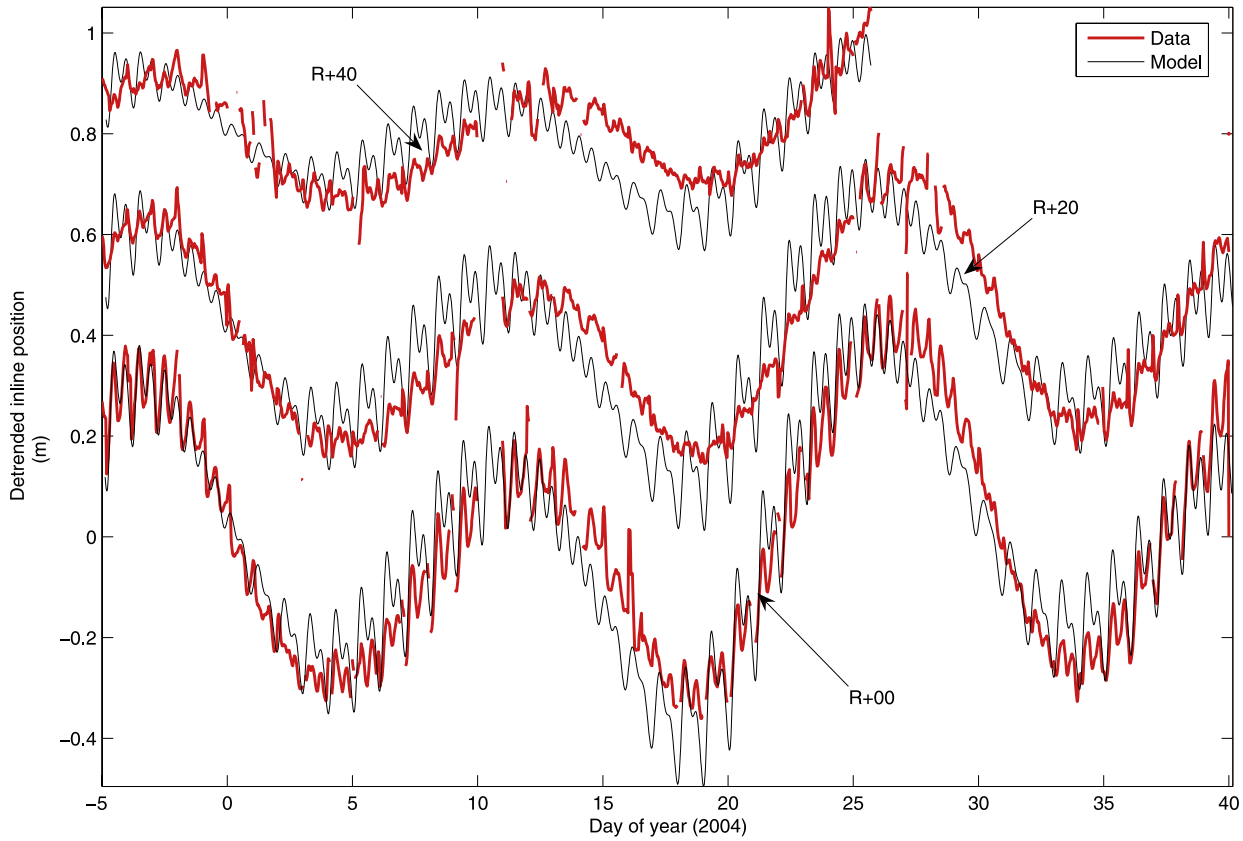

Figure 2. Measured (thick red lines) and modeled (thin black lines) detrended in-line positions for GPS stations R+00, R+20, and R+40. The curves have been offset by an arbitrary distance for clarity. In-line positions are defined as positions along mean flow direction.

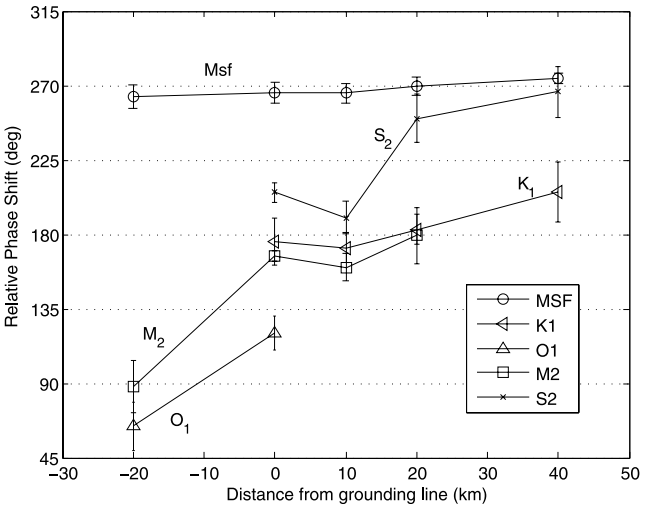

Figure 3. Phase difference between measured detrended in-line displacements and modeled vertical ocean tides. These curves were calculated by determining (for each tidal constituents) the absolute phases of (1) the horizontal detrended in-line displacements at all GPS sites and (2) the vertical ocean tide as predicted by the tidal model CATS02.01 [*Robertson et al.*, 1998]. Shown is the difference between the two. The phase calculations were done using the t_tide software package [*Pawlowicz et al.*, 2002]. The M_2 and S_2 are semidiurnal principal lunar and principal solar constituents, respectively, while K_1 and O_1 are diurnal lunar-solar and principal lunar constituents. The M_{sf} is the lunisolar synodic fortnightly tide. Error bars are 95% confidence intervals based on of the bootstrap method. Only phases of statistically significant tidal constituents are shown.

are plotted as functions of distance from the grounding line (positive distance in the upstream direction).

[7] Phase calculations were done using the t_tide software package [*Pawlowicz et al.*, 2002]. Phases shown in Figure 3 are statistically significant at 95% level. Only tidal constituents separated over the measurement period by at least one complete cycle from their neighboring constituents (Rayleigh criterion) were included in the tidal analysis. For this reason only either the M_{sf} (Lunisolar synodic fortnightly) or the M_f (Lunisolar fortnightly) constituent could be included in the analysis, and somewhat arbitrarily the M_{sf} was selected. The periods of the M_f and the M_{sf} tides are 13.66 and 14.76 days, respectively. (Note that in the work by *Gudmundsson* [2006] I got these numbers mixed up and mistakenly gave the period of the M_{sf} tide as that of the M_f tide.)

[8] Ocean tides were calculated using the CATS02.01 tidal model [*Padman et al.*, 2002; *Robertson et al.*, 1998]. These modeled ocean tides were compared with measured vertical positions and the agreement found to be excellent. The root-mean-square value of the difference between measured and the modeled tides was 0.18 m and the correlation coefficient was equal to 0.9901.

[9] At the grounding line the phases of the semidiurnal principal lunar (M_2) and principal solar (S_2), and those of the diurnal lunar-solar (K_1) and the principal lunar constituents (O_1) are around 180 degrees out of phase with the corresponding vertical ocean tide (Figure 3). This implies maximum horizontal in-line displacement in upstream direction during a high tide, or in terms of the velocities of these tidal constituents, a maximum downstream velocity coinciding with the falling tide. Further upstream, the phase relationship of the diurnal, and in particular that of the semidiurnal principal solar tide, changes gradually to 270 degrees. This corresponds to a situation where maximum forward velocities coincide with a high tide. Note that at R+40 the principal lunar semidiurnal tide (M_2) is no longer statistically significant. The phase of the lunisolar synodic fortnightly tide (M_{sf}) increases slowly with distance from the grounding line but is always around 270 degrees. This corresponds to highest and lowest velocities during spring and neap tides, respectively.

3. Model

[10] The increase in velocity leading up to an ocean spring tide and the subsequent velocity decrease toward an ocean neap tide, suggests that the velocity perturbation is related to changes in the peak-to-peak amplitudes of the semidiurnal tide, implying a nonlinear system response. The question arises as to what could be the source of this nonlinearity.

[11] The forward motion of an ice stream is mostly due to till deformation with the deformation of ice playing an insignificant role in comparison. The basal sliding velocity is generally expected to be some function of basal shear stress [*Clarke*, 1987; *Truffer*, 1999; *Iverson et al.*, 1995; *Tulaczyk et al.*, 2000; *Fischer et al.*, 2001; *Tulaczyk*, 2006], and this function is presumably nonlinear [*Hindmarsh*, 1997]. If stresses set up by tides are transmitted upstream of the grounding line, and are large enough compared to the mean basal shear stress to significantly affect the stresses within the till, a tidally induced modulation of the basal sliding velocity will result. For linear elastic ice, the tidal stresses are linearly related to tidal amplitude, and therefore the resulting perturbations in basal shear stress are linearly proportional to tidal amplitude as well. For a nonlinear relationship between basal sliding velocity and basal shear stress, the magnitude of the resulting perturbation in sliding velocity will, in general, differ between high and low tide. An amplitude-dependent net perturbation (i.e., over a whole diurnal/semidiurnal tidal cycle) in basal sliding velocity; thus results and velocities during a spring and neap tides will differ.

[12] To test this basic idea the basal shear stress, τ_b, is written as $\tau_b = \bar{\tau}_b + \Delta\tau_b(t)$, with

$$\Delta\tau_b(t) = K\rho_w g h(t), \tag{1}$$

that is,

$$\tau_b = \bar{\tau}_b + K\rho_w g h(t), \tag{2}$$

where $\bar{\tau}_b$ is the mean basal shear stress, ρ_w is the density of seawater, g the gravitational acceleration, and $h(t)$ the time varying ocean tide.

[13] Equation (1) expresses the assumption that the perturbation in basal stress is linearly related to tidal amplitude.

The parameter K is the constant of proportionality between the tidally related hydrostatic pressure variation ($\rho_w g h(t)$) and the resulting perturbation in basal shear stress at each measurement site upstream from the grounding line. K is therefore a site-dependent modeling parameter and its value is determined through model optimization.

[14] The basal motion, u_b, is assumed to be given by

$$u_b = C\,\tau_b^m, \tag{3}$$

where C and m are further modeling constants. This power law relationship between basal shear stress and sliding velocity is commonly used in glaciology and referred to as Weertman's sliding law [*Paterson*, 1994]. The total forward surface velocity (u_s) is

$$u_s = u_d + u_b = (1/c + 1)u_b, \tag{4}$$

where $c = u_b/u_d$ is the slip ratio, that is the ratio between mean sliding velocity and mean forward deformational velocity (u_d).

[15] Equation (2) is inserted into equation (3), which in turn is inserted into equation (4). The displacement as a function of time is then determined by forward integration of equation (4) using the measured vertical tides on R-20 as the tidal amplitude $h(t)$ in equation (1).

[16] Figure 2 shows comparison between modeled and measured detrended in-line positions (thin black lines). The values of the model parameters are: $m = 3.04$, slip ratio $r = 107$, $\bar{\tau}_b = 21$ kPa, $C = 0.12 \times 10^{-3}$ m d^{-1} kPa^{-m} and K was 0.27, 0.21, and 0.16 at locations R+00, R+20, and R+40, respectively. The solid black line in Figure 2 shows the modeled detrended in-line displacement. This set of parameter values is not unique, and within limits different parameter sets can give similarly good fit. From Figure 2 it can be concluded that despite the model's simplicity, and the fact that none of the elements of the model can be considered to as be novel or unexpected, i.e., elastic ice and viscous till, the model is capable of reproducing the fortnightly variations in flow (red curves) in considerable detail.

[17] The fortnightly variation in flow, as predicted by the model, is a consequence of the assumption of nonlinear till rheology. For $m = 1$ no fortnightly flow variations result. For $m > 1$ a positive perturbation in shear stress gives rise to an increase in basal motion which is larger than the decrease, resulting from equally large but negative shear stress perturbation. Furthermore, the magnitude of this imbalance between positive and negative perturbations in basal motion over a single tidal cycle, increases with increasing peak-to-peak tidal amplitude of the ocean tide. As as consequence, flow speeds are higher during a spring tide than a neap tide and a fortnightly variation in flow speed results.

[18] A further nonlinear effect is a net increase in mean flow velocity over each tidal cycle. For the particular set of model parameters given above, this effect gives about 5% increase in ice flux across the grounding line.

[19] The model gives rise to a fortnightly variations in flow even when forced with the semidiurnal S_2 and M_2 tides only. Such a nonlinear interaction between the S_2 and the M_2 tidal forcing results in a fortnightly tide with the same period as the M_{sf} tide, i.e., 14.76 days. Thus there is no need for any fortnightly component in the ocean tidal forcing in order to produce the fortnightly variation in the flow of the ice stream.

4. Discussion

4.1. Are Derived Values of Model Parameters Reasonable?

[20] The good fit between data and model output is promising. As no constraints were imposed on the values of model parameters during the model optimization, it remains however to be investigated if the above listed values of model parameters are within realistic bounds. Estimates of most model parameters can be done independently of model optimization as follows.

[21] From the average slope and thickness, and measured surface velocity, the slip ratio (c) of Rutford Ice Stream can be estimated to be $O(100)$. From this it follows that $u_d \ll u_s$, and the value of the sliding coefficient C is effectively determined by the mean surface velocity. This leaves the sliding exponent m, the local stress ratio K, and the mean basal shear stress $\bar{\tau}_b$ as adjustable model parameters. Driving stress (τ_d) is estimated from a surface slope ($\alpha = 0.0017$) and thickness ($h = 2200$ m) giving $\tau_d = 33$ kPa. Surface speed of a frictionless ice stream is related to driving stress, basal shear stress (τ_b), thickness (h), surface speed (u), and width (w) through

$$u = \frac{2A}{n+1} h(\tau_d - \tau_b)^n \left(\frac{w}{2h}\right)^{n+1},$$

where A and n are material parameters [*Raymond*, 1996]. It follows that $\tau_b = 21$ kPa for surface speed of 1 m d^{-1} and width of 25 km. This happens to be exactly the value obtained through model optimization. Although this is to some extent fortuitous, it is nevertheless good agreement.

[22] The value of the site-dependent parameter K is more difficult to estimate independently of the model as it requires an estimate of both the magnitude of stresses set up within the ice, and the spatial scale of stress transmission. The ocean tides exert a force on the ice shelf which acts in both horizontal and vertical directions. Assuming that the grounding line does not migrate with the tide, the vertically integrated horizontal force results in a horizontal stress (σ_{xx}) of $\rho_w g h(t)$ [*Anandakrishnan and Alley*, 1997]. In what follows, these stresses will referred to as hydrostatic stresses. Note that at high tide, hydrostatic stresses are negative (compressive) throughout the ice thickness. Tidally induced migration of the grounding line can be estimated to give rise to a force perturbation of similar magnitude but with an opposite sign [*Anandakrishnan and Alley*, 1997]. Given the bedrock geometry of Rutford Ice Stream [*Jenkins et al.*, 2006], significant tidally related migration of the grounding line of Rutford Ice Stream seems unlikely, and this possibility is discarded.

[23] The vertical force gives rise to viscoelastic flexure of the ice shelf. This is a well known and well studied process [*Lingle et al.*, 1981; *Doake et al.*, 1987; *Smith*, 1991; *Vaughan*, 1995; *Reeh et al.*, 2000; *Reeh*, 2003]. The resulting stresses set up within the ice shelf can be estimated using beam theory giving

$$\Delta\sigma_{xx} = 3\rho_w g h \lambda^2 H^{-2},$$

where $\Delta\sigma_{xx}$ is the basal horizontal stress perturbation at the grounding line, H the ice thickness, and λ the damping length [*Holdsworth*, 1969]. These stresses will be referred to as flexure stresses. For Rutford Ice Stream the value of λ has been estimated to be 4.2 km [*Vaughan*, 1995] by fitting measured data to a tidal flexure model. For an ice thickness of 1800 m, the above equation gives $\sigma_{xx} = 16.3\ \rho_w g h(t)$. Thus maximum flexure stresses are about 16 times larger in magnitude than the hydrostatic ones. For a tidal amplitude of 4 m, which is a typical tidal amplitude during a spring tide, the corresponding flexure stresses are about 650 kPa. This is large in comparison with the estimated basal shear stress of about 21 kPa.

[24] The values of the site-dependent parameter K are around 0.2, or about 20% of the hydrostatic stresses. Ignoring contribution from the margins, a simple force balance estimate gives a basal shear stress perturbation due to hydrostatic stresses equal to $-\rho_w g h(t)\ H/L$ where L is the distance over which basal stresses are noticeably disturbed. For Rutford Ice Stream L is larger than 40 km so $H/L < 0.045$, and a value of K around 0.2 therefore seems suspiciously large, beside the obvious fact that the sign is wrong. Thus either the model is wrong, or the basal shear stress perturbation upstream of the grounding line is not primarily related to the hydrostatic force. The latter possibility seems likely as this problem is fully resolved as soon as the much larger flexure stresses are considered. For the above listed range of values for K, the modeled maximum basal stress perturbation is only 1 to 1.7% of the grounding line values of maximum flexure stresses. Furthermore, now the signs of K are correct if it is assumed, as seems likely, that the flexure stresses along the lower boundary are not reversed as the grounding line is crossed.

[25] The proposed model assumes, as do other models that have been proposed to explain tidally modulated motion on ice streams [e.g., *Bindschadler et al.* 2003a], transmission of stresses upstream from the grounding line over distances that are long compared to mean ice thickness. The distance over which horizontal stresses are transmitted on glaciers and ice sheets depends critically on the slip ratio, i.e., the ratio between mean basal motion and mean forward deformational velocity [*Gudmundsson*, 2003]. For slip ratios typical of active ice streams, the theoretical spatial scale of stress transmission is a few hundred to a few thousand times the mean ice thickness, if the effects of side margins are ignored [*Gudmundsson*, 2003]. As the widths of ice streams are usually smaller than these numbers, the scale of horizontal stress transmission is effectively determined by the width of the ice stream and not the thickness. Rutford Ice Stream has a width of about 25 km, and assuming stress transmission over 100 km is therefore in no contradiction with theory.

[26] The assumption of linear viscoelastic behavior of ice over periods of a whole tidal cycle is investigated in Appendix A using a four element (Burgers) viscoelastic rheological model. It is found that ice at the surface is in fact expected to behave elastically over the whole spring-neap tidal cycle, and the basal ice elastically with respect to semidiurnal tides. Presumably the best available evidence for linear elastic behavior comes from *Jenkins et al.* [2006] who performed direct measurements temporal variation in strain with depth downstream of the grounding line of Rutford Ice Stream. They found strains to be linearly related to tidal amplitude.

[27] It can thus be concluded that, apart from the parameter m for which no good independent estimate is available, the values of all derived model parameters are within the bounds of expectation. The parameter m is clearly fundamental to ice stream dynamics as it determines the sensitivity of basal motion to shear stress, and from the model optimization an independent estimate of m has been given. Although the model could in principle be used to estimate possible ranges for all parameters and their mutual dependencies, no such attempt was made. Given the simplicity of the model, and the fact that basal conditions on Rutford Ice Stream are expected to be highly heterogeneous [*Smith*, 1997; *Vaughan et al.*, 2003] such an attempt seems premature.

4.2. Model Shortcomings

[28] The fact that model optimization results in parameter estimates that are all within the expected ranges gives added confidence in the validity of the model, and the basal shear stress estimate of 21 kPa is also comparable with estimates derived from inversion of satellite observations [*Joughin et al.*, 2006]. However, although the model reproduces the fortnightly variation in considerable detail, some aspects of the semi and diurnal variations are not reproduced by the model. For example the phase of the lunisolar synodic fortnightly constituent (M_{sf}) increases with distance upstream from the grounding line. This is manifested in Figure 2 through the misalignment between measured detrended inline positions from different measurement sites and can also be seen directly in Figure 3. This change in phase is not explained by the model. A possible explanation for this variation in phase with distance from the grounding line is a stress wave within the till traveling upstream as modeled by *Anandakrishnan et al.* [2003], or, alternatively, it is indicative of viscoelastic tidal flexure [*Reeh*, 2003]. The assumption of stresses within the ice being both instantaneously and linearly related to amplitude ignores any possible viscoelastic effects, and consequently the model cannot produce the observed variation in M_{sf} phase with distance. However, the model does predict a constant phase shift of 270 degrees which is within about 10 degrees of the actual measured phase shift at all locations (see Figure 3). The observed spatial variation in phase corresponds to a speed of about of 1 m s^{-1}. This speed is of the same order of magnitude as the both the 5.6 m s^{-1} observed velocity of upstream propagation of diurnal flow variations seen on Bindschadler Ice Stream [*Anandakrishnan et al.*, 2003], and the measured speed of tidal forcing of 1.6 m s^{-1} on Kamb Ice Stream [*Anandakrishnan and Alley*, 1997], but is much slower than the 88 ± 79 m s^{-1} propagation of stick-slip events on the ice plain of Whillans Ice Stream [*Bindschadler et al.*, 2003a].

[29] Around the grounding line, elastic flexure theory predicts longitudinal compression along the surface during high tide [*Holdsworth*, 1969]. Consequently, a local temporal minimum in surface velocity is expected to coincide with maximum rate of rising tide. This elastic effect is clearly seen in the data at R+00 and, understandably, much less so at R+20 (see Figure 2). Similar observations have been made on the grounding line of Bindschadler Ice

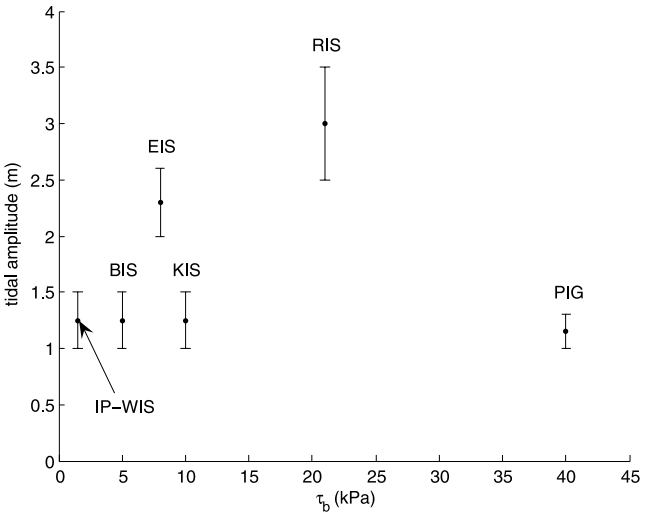

Figure 4. Basal shear stress (τ_b) and tidal amplitude at spring tide for a number of West Antarctica ice streams. Abbreviations used are PIG for Pine Island Glacier, RIS for Rutford Ice Stream, KIS for Kamb Ice Stream, EIS for Evans Ice Stream, BIS for Bindschadler Ice Stream, and IP-WIS for the ice plain of Whillans Ice Stream. Basal shear stresses given are approximates, and true basal shear stresses vary significantly within each ice stream [*Joughin et al.*, 2004]. Tidal ranges were calculated using the CATS02.01 tidal model [*Robertson et al.*, 1998] (see http://www.esr.org/ptm_index.html). Basal shear stress estimates are derived from *Raymond* [2000] and *Joughin et al.* [2004].

Stream [*Anandakrishnan et al.*, 2003]. This elastic effect is not accounted for in the model.

[30] According to the model, rates of (viscous) basal motion are expected to be largest at high tide. This viscous till effect is therefore not in phase with the elastic effect mentioned above. It follows that these two processes (viscous till/upstream elastic propagation) can be expected to partly work against each other over semidiurnal and diurnal timescales where elastic effects are important. As the elastic effect is not accounted for in the model, deconstructive interference of this type possibly explains why the model overestimates the semidiurnal and diurnal variation (see Figure 2).

4.3. Implications for Other Ice Streams

[31] The modeled strength of the fortnightly flow variation depends primarily on the size of the tidally induced basal shear stress perturbation in relation to the mean basal shear stress. The larger the tidal range is, and smaller the mean basal shear stress, the bigger the fortnightly flow variation. The temporal frequency of the stress perturbation is clearly also important. Thus semidiurnal tides, the dominant tides in the Ronne-Filchner embayment, are more likely to give rise to fortnightly flow variations than diurnal tides, which are the dominant tides under the Ross Ice Shelf. Figure 4 shows tidal range versus basal shear stress for a number of West Antarctic ice streams. Assuming all other factors are equal, ice streams subjected to similar tidal ranges and having equal or smaller basal shear stresses can be expected to exhibit fortnightly variations in flow of the type seen of Rutford Ice Stream. From Figure 4 it can be seen that Evans Ice Stream, which has the largest discharge of all ice streams flowing into Filchner-Ronne Ice Shelf, is a likely further candidate for showing fortnightly variations in flow as it is subjected to similar tidal amplitudes as the Rutford Ice Stream but has a smaller basal shear stress [*Vaughan et al.*, 2003].

[32] Observations of tidally induced flow variations on the Siple Ice Coast ice streams differ in number of ways from those of Rutford Ice Stream. On Bindschadler Ice Stream velocity fluctuation are, for example, diurnal with no reported fortnightly variation. The question arises as to whether this is due to differences between ice streams or differences in tidal forcing. Amplitudes of the diurnal tides of the grounding line of Bindschadler Ice Stream are only about 0.5 m [*Anandakrishnan and Bentley*, 1993], considerably smaller than the 4–5 m semidiurnal tidal amplitude at the grounding line of Rutford Ice Stream. Model runs using diurnal tides similar to those to which Bindschadler Ice Stream is subjected to as forcing, while keeping all other modeling parameters for Rutford Ice Stream, showed that the fortnightly variation is strongly reduced and becomes smaller than the diurnal one. The implication is therefore that if Rutford Ice Stream were subjected to the same type of tidal forcing as Bindschadler Ice Stream, it would primarily exhibit semidiurnal variations much in line with what is observed on Bindschadler Ice Stream. The simple model presented here therefore suggests that these differences could be mostly due to differences in forcing.

[33] Of particular importance are the implications of this model for other ice streams draining into Filchner-Ronne Ice Shelf (FRISP) as these are subjected to similar tidal range as Rutford Ice Stream [*Robertson et al.*, 1998]. It follows that the FRISP ice streams are expected to exhibit the same type of fortnightly flow variation, and this has consequences for the mass balance of the catchment area. Because of the nonlinear coupling between tides and rates of basal motion described above, tides can significantly affect the mean flow velocity of ice streams. For the particular set of parameter values given above, a few percent of the forward motion of Rutford Ice Stream is due to this effect. A further modeling effort is needed to clarify the magnitude of this effect.

5. Summary

[34] A simple conceptual model has been shown to be able to reproduce observations of fortnightly variations in flow of Rutford Ice Stream in considerable detail. The model assumes that elastic stresses set up by the tides are able to significantly perturb the basal shear stress distribution upstream of the grounding line. This requires both a long-range stress transmission within the ice, and large tidally induced stresses as compared with the mean basal shear stress. The long-range stress transmission seems justified given the high slip ratio of Rutford Ice Stream, which theoretically implies a transmission of horizontal deviatoric stresses over distances of a few times the ice stream width. The magnitude of tidally induced stresses is estimated using beam theory and it is found that these are large as compared to mean basal shear stress estimates. A

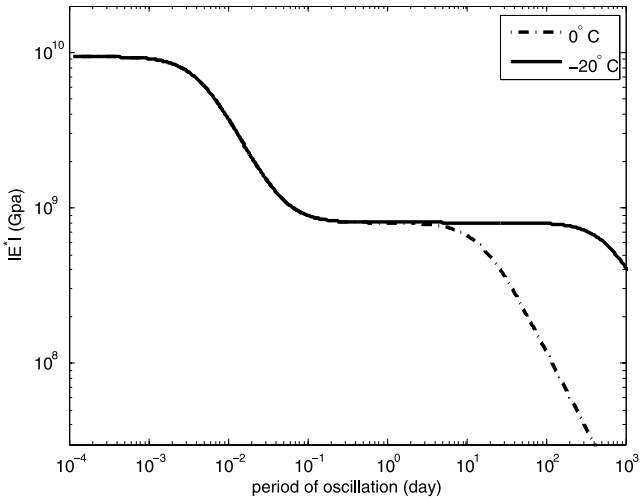

Figure A1. Magnitude of the complex elastic relaxation modulus ($|E^*|$) of a four-element fluid (Burgers model) as functions of forcing period for ice temperature of −20°C (solid line) and 0°C (dash-dotted line). Where the slope of complex modulus is zero, the response of ice is elastic, and nonzero slope indicates viscous response. For very short loading times, the response is elastic with modulus equal to the instantaneous Young's modulus of ice. For very long loading times, ice behaves as viscous material with an effective viscosity related to englacial temperature and effective stress. Between those two limits, there is a range of loading periods for which the ice behaves elastically but with a Young's modulus related to delayed elastic response (primary creep). The upper limit of this range depends strongly on englacial temperature.

further model assumption is that of nonlinear viscous till deformation. This assumption introduces a simple, but effective, nonlinear system response giving rise to an imbalance between positive and negative contribution to till deformation when integrated over one tidal cycle. The magnitude of this imbalance, in turn, depends on tidal amplitude, being larger during a spring tide than during a neap tide. It is found that, with the use of a realistic set of modeling parameters, this mechanism produces fortnightly spring-neap tidal variations in flow of the type observed.

[35] Modeling shows that the size of the maximal tidal amplitude, as measured over a typical spring-neap tidal cycle, is critical in determining if a fortnightly variation in ice flow results. It follows that many, if not all, of the ice streams flowing into the Ronne-Filchner ice shelf can be expected to exhibit the same type of variation in flow with time. If so, it furthermore seems possible that the speeds of the whole of Ronne-Filchner ice shelf fluctuate in similar manner. Measurements are needed to verify this, and until this issue has been clarified caution must be exercised when interpreting velocity measurements over time intervals shorter than a few spring-neap tidal cycles.

Appendix A

[36] The viscoelastic response of ice to periodic forcing is estimated using a Burgers model. Using the same notation as *Reeh* [2003], the instantaneous Young's modulus is denoted by E_M, the viscosity related to steady creep by μ_M, and E_V and μ_V are the elastic modulus and viscosity associated with primary creep, respectively. Expressions for the complex modulus for the Burgers model can be found in any introductory textbooks to viscoelasticity [e.g., *Findley et al.*, 1976]. Measurements by *Röthlisberger* [1972] and least squares fit by *Hutter* [1983] give an instantaneous elastic Young's modulus at −20°C of 9.4 GPa. For Rutford Ice Stream the estimate of E_V = 0.88 GPa derived from flexure analysis [*Vaughan*, 1995] is used. *Brill and Camp* [1961] (as cited by *Reeh* [2003]) give μ_V on the order of 600 GPa s. The vertical temperature profile of Rutford Ice Stream is unknown, but surface temperatures are around −25°C and basal ice is at the pressure melting point. To bracket the possible range the complex modulus is plotted for both −20°C (solid line) and 0°C (dash-dotted line) using an effective stress of τ = 21 kPa. Values for the rate factor were taken from *Paterson* [1994]. The corresponding effective viscosity of ice is estimated as 6.6×10^{15} Pa s and 0.17×10^{15} Pa s at −20°C and 0°C, respectively. Using these values the magnitude of the complex modulus ($|E^*|$) is plotted in Figure A1. As can be seen from the Figure A1, ice at −20°C is predicted to show mostly viscous response for time periods between about 10 to 1000 sec, and again for periods above about 100 days. For time periods within about one hour to about 50 days, the response of the cold ice is almost purely elastic, while the warm ice reacts elastically for oscillations with periodicity up to about 1/2 day. It is concluded that ice at the surface behaves elastically over the whole spring-neap tidal cycle, and the basal ice elastically with respect to semidiurnal tides.

[37] **Acknowledgments.** This research was supported by NERC geophysical equipment loan 785. I thank R. C. A. Hindmarsh for discussions and interest in this project and two anonymous reviewers for helpful reviews.

References

Anandakrishnan, S., and R. B. Alley (1994), Ice Stream C, Antartica, sticky spots detected by microeathquake monitoring, *Ann. Glaciol.*, *20*, 183–186.

Anandakrishnan, S., and R. B. Alley (1997), Tidal forcing of basal seismicity of ice stream C, West Antarctica, observed far inland, *J. Geophys. Res.*, *102*, 15,183–15,196.

Anandakrishnan, S., and C. R. Bentley (1993), Micro-earthquakes beneath Ice Streams B and C, West Antarctica: Observations and implications, *J. Glaciol.*, *39*, 455–462.

Anandakrishnan, S., D. E. Voigt, R. B. Alley, and M. A. King (2003), Ice stream D flow speed is strongly modulated by the tide beneath the Ross Ice Shelf, *Geophys. Res. Lett.*, *30*(7), 1361, doi:10.1029/2002GL016329.

Bindschadler, R. A., M. A. King, R. B. Alley, S. Anandakrishnan, and L. Padman (2003a), Tidally controlled stick-slip discharge of a West Antartic ice stream, *Science*, *301*, 1087–1089.

Bindschadler, R. A., P. L. Vornberger, M. A. King, and L. Padman (2003b), Tidally driven stick-slip motion in the mouth of Whillans Ice Stream, Antarctica, *Ann. Glaciol.*, *36*, 263–272.

Brill, R., and P. R. Camp (1961), Properties of ice, *Res. Rep. 68*, Snow Ice and Permafrost Res. Estab., Hanover, N. H.

Clarke, G. K. C. (1987), Subglacial till: A physical framework for its properties and processes, *J. Geophys. Res.*, *92*, 9023–9036.

Doake, C. S. M., R. M. Frolich, D. R. Mantripp, A. M. Smith, and D. G. Vaughan (1987), Glaciological studies on Rutford Ice Stream, Antarctica, *J. Geophys. Res.*, *92*, 8951–8960.

Findley, W. N., J. S. Lai, and K. Onaran (1976), *Creep and Relaxation of Nonlinear Viscoelastic Materials*, Dover, Mineola, N. Y.

Fischer, U. H., P. R. Porter, T. Schuler, A. J. Evans, and G. H. Gudmundsson (2001), Hydraulic and mechanical propeties of glacial sediments beneath Unteraargletscher, Switzerland: Implications for glacier basal motion, *Hydrol. Processes*, *15*, 3525–3540, doi:10.1002/hyp.349.

Gudmundsson, G. H. (2003), Transmission of basal variability to a glacier surface, *J. Geophys. Res.*, *108*(B5), 2253, doi:10.1029/2002JB002107.
Gudmundsson, G. H. (2006), Fortnightly variations in the flow velocity of Rutford Ice Stream, West Antarctica, *Nature*, *444*(7122), 1063–1065.
Harrison, W. D., K. A. Echelmeyer, and H. Engelhardt (1993), Short-period observations of speed, strain and seismicity on Ice Stream B, Antarctica, *J. Glaciol.*, *39*, 463–470.
Hindmarsh, R. C. A. (1997), Deforming beds: Viscous and plastic scales of deformation, *Quat. Sci. Rev.*, *16*(9), 1039–1056.
Holdsworth, G. (1969), Flexure of a floating ice tongue, *J. Glaciol.*, *8*, 385–397.
Hugentobler, U., R. Dach, P. Fridez, and M. Meindl (Eds.) (2006), Bernese GPS software version 5.0, Print. Off. of the Univ. of Bern, Bern.
Hutter, K. (1983), *Theoretical Glaciology: Material Science of Ice and the Mechanics of Glaciers and Ice Sheets*, Springer, New York.
Iverson, N. R., B. Hanson, R. L. Hooke, and P. Jansson (1995), Flow mechanism of glaciers on soft beds, *Science*, *267*(5194), 80–81.
Jenkins, A., H. F. J. Corr, K. W. Nicholls, C. L. Stewart, and C. S. M. Doake (2006), Interactions between ice and ocean observed with phase-sensitive rader near an Antarctic ice-shelf grounding line, *J. Glaciol.*, *52*, 325–346.
Joughin, I., D. R. MacAyeal, and S. Tulaczyk (2004), Basal shear stress of the Ross ice streams from control method inversions, *J. Geophys. Res.*, *109*, B09405, doi:10.1029/2003JB002960.
Joughin, I., J. L. Bamber, T. Scambos, S. Tulaczyk, M. Fahnestock, and D. R. MacAyeal (2006), Integrating satellite observations with modeling: Basal shear stress of the Filcher-Ronne Ice Stream, Antarctica, *Proc. R. Soc. London, Ser.*, *364*(1844), 1795–1814, doi:10.1098/rsta.2006.1799.
King, M. A. (2004), Rigorous GPS data-processing strategies for glaciological applications, *J. Glaciol.*, *50*, 601–607.
King, M., L. Nguyen, R. Coleman, and P. J. Morgan (2000), Strategies for high precision processing of GPS measurements with application to the Amery Ice Self, East Antarctica, *GPS Solutions*, *4*(1), 2–12.
Lingle, C. S., T. J. Hughes, and R. C. Kollmeyer (1981), Tidal flexure of Jakobshavns Glacier, West Greenland, *J. Geophys. Res.*, *86*, 3960–3968.
Padman, L., H. A. Fricker, R. Coleman, S. Howard, and L. Erofeeva (2002), A new tide model for the Antarctic ice shelves and seas, *Ann. Glaciol.*, *34*, 247–254.
Paterson, W. S. B. (1994), *The Physics of Glaciers*, 3rd ed., 480 pp., Pergamon, New York.
Pawlowicz, R., B. Beardsley, and S. Lentz (2002), Harmonic analysis including error estimates in MATLAB using T_TIDE, *Comput. Geosci.*, *28*, 929–937.
Raymond, C. F. (1996), Shear margins in glaciers and ice sheets, *J. Glaciol.*, *42*, 90–102.
Raymond, C. F. R. (2000), Energy balance of ice streams, *J. Glaciol.*, *46*, 665–674.
Reeh, N. (2003), Tidal bending of glaciers: A linear viscoelastic approach, *Ann. Glaciol.*, *37*, 83–89.
Reeh, N., C. Mayer, and O. Olesen (2000), Tidal movement of Nioghalvfjerdsfjorden glacier, northeast Greenland: Observations and modelling, *Ann. Glaciol.*, *31*, 111–117.
Robertson, R. A., L. Padman, and G. D. Egber (1998), Tides in the Weddell Sea, in *Ocean, Ice, and Atmosphere: Interactions at the Antarctic Continental Margin*, *Antarct. Res. Ser.*, vol. 75, edited by S. S. Jacobs and R. F. Weiss, pp. 341–369, AGU, Washington, D. C.
Röthlisberger, H. (1972), Seismic exploration in cold regions, *Tech. Rep. Monogr. II-A 20*, U.S. Army Cold Reg. Res. and Eng. Lab., Hanover, N. H.
Smith, A. M. (1991), The use of tilmeters to study the dynamics of Antarctic ice-shelf grounding lines, *J. Glaciol.*, *37*, 51–58.
Smith, A. M. (1997), Variations in basal conditions on Rutford Ice Stream, West Antarctica, *J. Glaciol.*, *43*, 245–255.
Truffer, M. (1999), Till deformation beneath Black Rapids Glacier, Alaska, and its implication on glacier motion, Ph.D. thesis, Univ. of Alaska Fairbanks, Fairbanks.
Tulaczyk, S. (2006), Scale independence of till rheology, *J. Glaciol.*, *52*, 377–380.
Tulaczyk, S., W. B. Kamb, and H. F. Engelhardt (2000), Basal mechanics of Ice Stream B, West Antarctica: 1. Till mechanics, *J. Geophys. Res.*, *105*, 463–482.
Vaughan, D. G. (1995), Tidal flexure at ice shelf margins, *J. Geophys. Res.*, *100*, 6213–6224.
Vaughan, D. G., A. M. Smith, and E. LeMeur (2003), Acoustic impedance and basal shear stress beneath four Antarctic ice streams, *Ann. Glaciol.*, *36*, 225–232.

G. H. Gudmundsson, British Antarctic Survey, High Cross, Madingley Road, Cambridge CB3 0ET, UK. (ghg@bas.ac.uk)